Article

Dispersion and Dampingof Phononic Excitations in Fermi Superfluid Gases in2D

Lars-Paul Lumbeeck [1], Jacques Tempere [1,2] and Serghei Klimin [1]*

[1] TQC, Universiteit Antwerpen, Universiteitsplein 1, B-2610 Antwerpen, Belgium
[2] Lyman Laboratory of Physics, Harvard University, Cambridge, Massachusetts MA 02138, USA
* Correspondence: sergei.klimin@uantwerpen.be

Abstract: We calculate the sound velocity and the damping rate of the collective excitations of a 2D fermionic superfluid in a non-perturbative manner. Specifically, we focus on the Anderson-Bogoliubov excitations in the BEC-BCS crossover regime, as these modes have a soundlike dispersion at low momenta. The calculation is performed within the path integral formalism and the Gaussian pair fluctuation approximation. From the action functional, we obtain the propagator of the collective excitations and determine their dispersion relation by locating the poles of this propagator. We find that there is only one kind of collective excitation, which is stable at $T = 0$ and has a sound velocity of $v_F/\sqrt{2}$ for all binding energies, i.e. throughout the BEC-BCS crossover. As the temperature is raised, the sound velocity decreases and the damping rate shows a non-monotonous behavior: after an initial increase, close to the critical temperature T_C the damping rate decreases again. In general, higher binding energies provide higher damping rates. Finally, we calculate the response functions and propose that they can be used as another way to determine the sound velocity.

Keywords: quantum gases; collective excitations; sound velocity

1. Introduction

Collective excitations in ultracold atomic Fermi gases are a subject of intense experimental [1–8] and theoretical [10–14] research, because their spectra provide valuable information on the internal states of the atomic system. In recent works [12–14], the eigenfrequencies and damping rates of different collective excitations (phonons, pair-breaking "Higgs"modes, Leggett modes) have been calculated in a non-perturbative way within the Gaussian pair fluctuation (GPF) approach based on the GPF effective bosonic action [15–17]. These studies are related to fermionic systems in three dimensions. Because the experimental setup for cold atomic gases made it possible to reach highly anisotropic trapping of atoms, an effectively two-dimensional geometry is at present experimentally achievable. It makes theoretical investigations of collective excitations of ultracold quantum gases in two dimensions timely and relevant.

The purpose of this study is to investigate the dispersion relation of collective excitations of a 2D fermionic superfluid without making the assumption that the damping rate is small enough to treat perturbatively. In this sense we refer to our method as "non-perturbative", to contrast it with previous treatments. Nevertheless it must be kept in mind that the Gaussian pair fluctuation approach itself still relies on a fluctuation expansion around a self-consistent mean-field. Here, we specifically focus on Anderson-Bogoliubov excitations [9–11], characterized by their sound-like dispersion relationship at low momenta.

2. Gaussian Pair Fluctuation Approximation

In the path integral formalism [18] the partition sum of a quantum field $\psi_{\mathbf{x},\tau,\sigma}$ (that depends on position $\mathbf{x}$, imaginary time τ and spin σ) is obtained by summing all possible field configurations, where and each field configuration is weighted by a factor $e^{-S[\{\bar{\psi}_{\mathbf{x},\tau,\sigma},\psi_{\mathbf{x},\tau,\sigma}\}]}$, with $S[\{\bar{\psi}_{\mathbf{x},\tau,\sigma},\psi_{\mathbf{x},\tau,\sigma}\}]$ is the action functional of the system under investigation.

Our calculations start with the action functional for an ultra-cold Fermi gas [15–17]. Ultra-cold means that the thermal wavelength of the atomic gas is large compared to the range of the interatomic potential, so that it can be approximated by a contact potential: $V(\mathbf{r}-\mathbf{r}') = g\delta(\mathbf{r}-\mathbf{r}')$. Because of the fermionic anti-symmetry requirement, s-wave interactions can only occur between opposite-spin fermions. Hence, the action potential is given by

$$S\left[\bar{\psi},\psi\right] = \int_0^{\hbar\beta} d\tau \int d\mathbf{x} \sum_\sigma \left(\bar{\psi}_{\mathbf{x},\tau,\sigma}\hbar\frac{\partial}{\partial\tau} - \frac{\hbar^2}{2m}\nabla_{\mathbf{x}}^2 - \mu_\sigma \right) \psi_{\mathbf{x},\tau,\sigma} + g\int_0^{\hbar\beta} d\tau \int d\mathbf{x}\, \bar{\psi}_{\mathbf{x},\tau,\uparrow}\bar{\psi}_{\mathbf{x},\tau,\downarrow}\psi_{\mathbf{x},\tau,\downarrow}\psi_{\mathbf{x},\tau,\uparrow}, \tag{1}$$

with m the mass of the atoms and $\beta = 1/(k_B T)$ with T the temperature. The fermionic fields $\psi_{\mathbf{x},\tau,\uparrow}$ and $\bar{\psi}_{\mathbf{x},\tau,\downarrow}$ are Grassmann variables, and the number of spin-up and spin-down atoms ($\sigma = \uparrow,\downarrow$) is determined by the chemical potentials $\mu_\uparrow$ and $\mu_\downarrow$. Here, we restrict ourselves to balanced fermi gases (equal amounts of spin-up and spin-down particles), so that there is only one chemical potential $\mu = \mu_\downarrow = \mu_\uparrow$. The strength of the contact potential is determined by the parameter g. For a two-dimensional atomic gas it can be related to the binding energy E_b of the atoms, such that [19]:

$$\frac{1}{g} = \frac{1}{8\pi}(i\pi - \ln(E/E_b)) - \int_0^{+\infty}\frac{kdk}{2\pi}\frac{1}{2k^2 - E + i\epsilon}. \tag{2}$$

At low temperature and low binding energy $0 < E_b < 2E_F$, the two-dimensional Fermi gas is in the Bardeen-Cooper-Schrieffer regime of superfluidity, whereas for $E_b > 2E_F$ it is in the Bose-Einstein quasi-condensate regime of tightly bound pairs. Here, we choose units such that $\hbar, 2m, k_F, k_B = 1$ (so that $E_F = 1$ as well). These are essentially density based units: since $k_F = \sqrt{2\pi n}$, the total density n equals $1/(2\pi)$ in our units. Note that the Fermi velocity in these units equals $v_F = (\hbar k_F)/m = 2$.

When fermionic pairing is present, it is convenient to introduce a bosonic field representing these pairs, by performing the Hubbard-Stratonovich transformation [20,21]. This transformation converts the partition sum to:

$$Z = \int \mathcal{D}\bar{\psi}_{\mathbf{k},n,\sigma}\mathcal{D}\psi_{\mathbf{k},n,\sigma}\int \mathcal{D}\bar{\Delta}_{\mathbf{q},m}\mathcal{D}\Delta_{\mathbf{q},m}\exp\left(\sum_{\mathbf{q},m}\frac{\bar{\Delta}_{\mathbf{q},m}\Delta_{\mathbf{q},m}}{g} - \sum_{\mathbf{k}',n'}\sum_{\mathbf{k}'',n''}\bar{\eta}_{\mathbf{k}',n'}\langle\mathbf{k}',n'|-\mathbb{G}^{-1}|\mathbf{k}'',n''\rangle\eta_{\mathbf{k}'',n''}\right) \tag{3}$$

with

$$\langle\mathbf{k},n|-\mathbb{G}^{-1}|\mathbf{k}',n'\rangle = \langle\mathbf{k}',n'|\mathbf{k}'',n''\rangle\begin{pmatrix} -i\omega_n + k^2 - \mu & 0 \\ 0 & i\omega_n - k^2 - \mu \end{pmatrix} + \frac{1}{\sqrt{\beta V}}\begin{pmatrix} 0 & -\Delta_{\mathbf{k}+\mathbf{k}',n+n'} \\ -\bar{\Delta}_{\mathbf{k}+\mathbf{k}',n+n'} & 0 \end{pmatrix} \tag{4}$$

and the Nambu spinors

$$\eta_{\mathbf{k},n} = \begin{pmatrix} \psi_{\mathbf{k},n,\uparrow} \\ \bar{\psi}_{\mathbf{k},n,\downarrow} \end{pmatrix}, \quad \bar{\eta}_{\mathbf{k},n} = \begin{pmatrix} \bar{\psi}_{\mathbf{k},n,\downarrow} & \psi_{\mathbf{k},n,\uparrow} \end{pmatrix}. \tag{5}$$

Here, $\omega_n = 2\pi n/\beta$ are the fermionic Matsubara frequencies ($n \in \mathbb{Z}$) and $\mathbf{k} = \{k_x, k_y\} = (2\pi/L)\{n_x, n_y\}$ (with $n_x, n_y, n_z \in \mathbb{Z}$). The bosonic scalar pair fields are $\bar{\Delta}_{\mathbf{q},m}$ and $\Delta_{\mathbf{q},m}$. When a uniform pair (quasi-)condensate is present, this implies that a macroscopic number of pairs occupy the same pair state: the quantum field can be approximated by a classical field Δ that is constant in space and imaginary time:

$$\Delta_{\mathbf{q},m} = \sqrt{\beta V}\delta(\mathbf{q})\delta_{m,0}\Delta, \quad \bar{\Delta}_{\mathbf{q},m} = \sqrt{\beta V}\delta(\mathbf{q})\delta_{m,0}\Delta^*. \tag{6}$$

With (6), the partition function becomes [22]:

$$Z_{sp} = e^{-\beta V \Omega_{sp}(T,\mu)} \tag{7}$$

where Ω_{sp} is the saddle-point (or mean-field) grand canonical thermodynamic potential,

$$\Omega_{sp} = -\frac{1}{g}|\Delta|^2 - \frac{1}{V}\sum_{\mathbf{k}}\left[\frac{1}{\beta}\ln\left[2\cosh\left(\beta E_{\mathbf{k}}\right) + 2\right] - \xi_{\mathbf{k}}\right] \tag{8}$$

with $\xi_{\mathbf{k}} = \mathbf{k}^2 - \mu$ and $E_{\mathbf{k}} = \sqrt{\xi_{\mathbf{k}}^2 + \Delta^2}$. The gap Δ must be determined self consistently: as a classical field solution, it must extremize the action. This leads to the gap equation:

$$\frac{1}{V}\sum_{\mathbf{k}}\left[\frac{1}{2E_{\mathbf{k}}}\tanh\left(\frac{\beta}{2}E_{\mathbf{k}}\right)\right] + \frac{1}{g} = 0. \tag{9}$$

Note that in two dimensions, the gap equation can be solved analytically with respect to Δ:

$$\Delta^2 = \frac{4}{\beta^2}\operatorname{arccosh}^2\left\{\frac{1}{2}\exp\left[\frac{\beta}{2}(2-\mu)\right]\right\} - \mu^2. \tag{10}$$

This solution must be supplemented with an equation for the chemical potential. Within the saddle-point approach, the particle density is given by

$$n_{sp} = -\frac{\partial\Omega_{sp}}{\partial\mu} = \int_0^{+\infty}\frac{kdk}{2\pi}\left[1 - \frac{\xi_{\mathbf{k}}}{E_{\mathbf{k}}}\tanh\left(\frac{\beta}{2}E_k\right)\right]. \tag{11}$$

The chemical potential is then obtained from setting $n_{sp} = 1/(2\pi)$.

To go beyond the saddle point approximation, we must restore the quantum fluctuations, adding them back to the classical field. The fluctuations around the saddle point can further be split into amplitude fluctuations $a_{\mathbf{q},z}$ and phase fluctuations $\theta_{\mathbf{q},z}$. Assuming that the classical field solution still dominates, the fluctuation fields are considered small so the action can be expanded to quadratic order in the fluctuation fields. This leads to a result for the partition sum that is mathematically similar to the result obtained for a superfluid Fermi gas in 3D [12,13]:

$$Z = Z_{sp}\int \mathcal{D}\theta_{\mathbf{q},z}\mathcal{D}a_{\mathbf{q},z}\exp\left[-\frac{1}{2}\sum_{\mathbf{q},z}\begin{pmatrix}\theta_{\mathbf{q},z}\Delta & a_{\mathbf{q},z}\end{pmatrix}\begin{pmatrix}M_{++}(z,\mathbf{q}) & -iM_{+-}(z,\mathbf{q}) \\ iM_{-+}(z,\mathbf{q}) & M_{--}(z,\mathbf{q})\end{pmatrix}\begin{pmatrix}\theta_{\mathbf{q},z}\Delta \\ a_{\mathbf{q},z}\end{pmatrix}\right]. \tag{12}$$

As the fluctuation action is quadratic in the fields, the matrix $\mathbb{M}$ with elements $M_{++}, \pm iM_{+-}, M_{--}$ represents the inverse propagator of the bosonic fluctuations. The matrix elements are given by:

$$M_{++}(z,\mathbf{q}) = \int \frac{d\mathbf{k}}{(2\pi)^2} \frac{X\left(E_{\mathbf{k}+\frac{\mathbf{q}}{2}}\right) + X\left(E_{\mathbf{k}-\frac{\mathbf{q}}{2}}\right)}{4E_{\mathbf{k}+\frac{\mathbf{q}}{2}}E_{\mathbf{k}-\frac{\mathbf{q}}{2}}} \frac{\left(E_{\mathbf{k}+\frac{\mathbf{q}}{2}}E_{\mathbf{k}-\frac{\mathbf{q}}{2}} + \xi_{\mathbf{k}+\frac{\mathbf{q}}{2}}\xi_{\mathbf{k}-\frac{\mathbf{q}}{2}} + \Delta^2\right)\left(E_{\mathbf{k}+\frac{\mathbf{q}}{2}} + E_{\mathbf{k}-\frac{\mathbf{q}}{2}}\right)}{z^2 - \left(E_{\mathbf{k}+\frac{\mathbf{q}}{2}} + E_{\mathbf{k}-\frac{\mathbf{q}}{2}}\right)^2}$$
$$+ \int \frac{d\mathbf{k}}{(2\pi)^2} \frac{X\left(E_{\mathbf{k}+\frac{\mathbf{q}}{2}}\right) - X\left(E_{\mathbf{k}-\frac{\mathbf{q}}{2}}\right)}{4E_{\mathbf{k}+\frac{\mathbf{q}}{2}}E_{\mathbf{k}-\frac{\mathbf{q}}{2}}} \frac{\left(E_{\mathbf{k}+\frac{\mathbf{q}}{2}}E_{\mathbf{k}-\frac{\mathbf{q}}{2}} - \xi_{\mathbf{k}+\frac{\mathbf{q}}{2}}\xi_{\mathbf{k}-\frac{\mathbf{q}}{2}} - \Delta^2\right)\left(E_{\mathbf{k}+\frac{\mathbf{q}}{2}} - E_{\mathbf{k}-\frac{\mathbf{q}}{2}}\right)}{z^2 - \left(E_{\mathbf{k}+\frac{\mathbf{q}}{2}} - E_{\mathbf{k}-\frac{\mathbf{q}}{2}}\right)^2}$$
$$+ \int \frac{d\mathbf{k}}{(2\pi)^2} \frac{X(E_{\mathbf{k}})}{2E_{\mathbf{k}}}, \tag{13}$$

$$M_{+-}(z,\mathbf{q}) = z\int \frac{d\mathbf{k}}{(2\pi)^2} \left[\frac{X\left(E_{\mathbf{k}+\frac{\mathbf{q}}{2}}\right) + X\left(E_{\mathbf{k}-\frac{\mathbf{q}}{2}}\right)}{4E_{\mathbf{k}+\frac{\mathbf{q}}{2}}E_{\mathbf{k}-\frac{\mathbf{q}}{2}}} \frac{\xi_{\mathbf{k}+\frac{\mathbf{q}}{2}}E_{\mathbf{k}-\frac{\mathbf{q}}{2}} + \xi_{\mathbf{k}-\frac{\mathbf{q}}{2}}E_{\mathbf{k}+\frac{\mathbf{q}}{2}}}{z^2 - \left(E_{\mathbf{k}+\frac{\mathbf{q}}{2}} + E_{\mathbf{k}-\frac{\mathbf{q}}{2}}\right)^2} \right.$$
$$\left. + \frac{X\left(E_{\mathbf{k}+\frac{\mathbf{q}}{2}}\right) - X\left(E_{\mathbf{k}-\frac{\mathbf{q}}{2}}\right)}{4E_{\mathbf{k}+\frac{\mathbf{q}}{2}}E_{\mathbf{k}-\frac{\mathbf{q}}{2}}} \frac{\xi_{\mathbf{k}+\frac{\mathbf{q}}{2}}E_{\mathbf{k}-\frac{\mathbf{q}}{2}} - \xi_{\mathbf{k}-\frac{\mathbf{q}}{2}}E_{\mathbf{k}+\frac{\mathbf{q}}{2}}}{z^2 - \left(E_{\mathbf{k}+\frac{\mathbf{q}}{2}} - E_{\mathbf{k}-\frac{\mathbf{q}}{2}}\right)^2} \right], \tag{14}$$

$$M_{--}(z,\mathbf{q}) = \int \frac{d\mathbf{k}}{(2\pi)^2} \left[\frac{X\left(E_{\mathbf{k}+\frac{\mathbf{q}}{2}}\right) + X\left(E_{\mathbf{k}-\frac{\mathbf{q}}{2}}\right)}{4E_{\mathbf{k}+\frac{\mathbf{q}}{2}}E_{\mathbf{k}-\frac{\mathbf{q}}{2}}} \frac{\left(E_{\mathbf{k}+\frac{\mathbf{q}}{2}}E_{\mathbf{k}-\frac{\mathbf{q}}{2}} + \xi_{\mathbf{k}+\frac{\mathbf{q}}{2}}\xi_{\mathbf{k}-\frac{\mathbf{q}}{2}} - \Delta^2\right)\left(E_{\mathbf{k}+\frac{\mathbf{q}}{2}} + E_{\mathbf{k}-\frac{\mathbf{q}}{2}}\right)}{z^2 - \left(E_{\mathbf{k}+\frac{\mathbf{q}}{2}} + E_{\mathbf{k}-\frac{\mathbf{q}}{2}}\right)^2} \right.$$
$$\left. + \frac{X\left(E_{\mathbf{k}+\frac{\mathbf{q}}{2}}\right) - X\left(E_{\mathbf{k}-\frac{\mathbf{q}}{2}}\right)}{4E_{\mathbf{k}+\frac{\mathbf{q}}{2}}E_{\mathbf{k}-\frac{\mathbf{q}}{2}}} \frac{\left(E_{\mathbf{k}+\frac{\mathbf{q}}{2}}E_{\mathbf{k}-\frac{\mathbf{q}}{2}} - \xi_{\mathbf{k}+\frac{\mathbf{q}}{2}}\xi_{\mathbf{k}-\frac{\mathbf{q}}{2}} + \Delta^2\right)\left(E_{\mathbf{k}+\frac{\mathbf{q}}{2}} - E_{\mathbf{k}-\frac{\mathbf{q}}{2}}\right)}{z^2 - \left(E_{\mathbf{k}+\frac{\mathbf{q}}{2}} - E_{\mathbf{k}-\frac{\mathbf{q}}{2}}\right)^2} + \frac{X(E_{\mathbf{k}})}{2E_{\mathbf{k}}} \right], \tag{15}$$

with the function

$$X(E_{\mathbf{k}}) = \tanh\left(\beta E_{\mathbf{k}}/2\right). \tag{16}$$

The bosonic excitations of the fermionic superfluid determine the poles of the propagator $\mathbb{M}^{-1}$. For fixed $\mathbf{q}$, the excitation energy is found as the real part of the pole and the damping rate as its imaginary part. Here, our goal is to extract the sound velocity and sound damping, so we focus on the long-wavelength behavior of the Anderson-Bogoliubov mode. The long-wavelength limit is found by setting $z = uq$ for the dispersion relation, and only after this substitution taking the limit $q \to 0$. We arrive at the result:

$$M_{--} = \int_0^\infty \frac{kdk}{4\pi} \left[\frac{\Delta^2 X(E_k)}{E_k^3} + \frac{\Delta^2 X'(E_k)}{E_k^2} \left(\sqrt{\frac{u^2}{u^2 - v_k^2}} - 1 \right) \right] + O\left(q^2\right), \tag{17}$$

$$M_{+-} = -uq \int_0^\infty \frac{kdk}{4\pi} \left[\frac{X(E_k)\xi_k}{2E_k^3} + \frac{\Delta^2 X'(E_k)}{2E_k^2\xi_k} \left(\sqrt{\frac{u^2}{u^2 - v_k^2}} - 1 \right) \right] + O\left(q^3\right), \tag{18}$$

$$M_{++} = q^2 \int_0^\infty \frac{kdk}{4\pi} \left[\frac{X(E_k)}{E_k^5} \left(-\frac{3}{2}\xi_k^2 k^2 + E_k^2 k^2 + \frac{1}{2}\xi_k E_k^2 - \frac{1}{4}u^2 E_k^2 \right) \right.$$
$$\left. + \frac{\Delta^2 X'(E_k) k^2}{E_k^4} \left((u/v_k)^2 \sqrt{\frac{u^2}{u^2 - v_k^2}} - \frac{1}{2} - (u/v_k)^2 \right) \right] + O\left(q^4\right). \tag{19}$$

where $X'(E_k) = dX(E_k)/dE_k$. In the long-wavelength limit, the matrix elements are a function of the parameter u. The sound mode is then found by identifying for which value of the complex u parameter the propagator has a pole. This comes down to solving $\det \mathbb{M}(u) = 0$. Using the long-wavelength

expansion (17)-(19), the determinant of the inverse fluctuation propagator can be simplified similarly to Ref. [13]:

$$\det \mathbb{M} = \left[U(u)\, C(u) - D^2(u)\right] q^2 + O\left(q^4\right), \tag{20}$$

where the coefficients for the 2D case are:

$$U(u) = \int_0^\infty \frac{kdk}{4\pi} \left[\frac{\Delta^2 X(E_k)}{E_k^3} + \frac{\Delta^2 X'(E_k)}{E_k^2}\left(\sqrt{\frac{u^2}{u^2 - v_k^2}} - 1\right)\right], \tag{21}$$

$$D(u) = -u \int_0^\infty \frac{kdk}{4\pi} \left[\frac{X(E_k)\,\xi_k}{2E_k^3} + \frac{\Delta^2 X'(E_k)}{2E_k^2 \xi_k}\left(\sqrt{\frac{u^2}{u^2 - v_k^2}} - 1\right)\right], \tag{22}$$

$$\begin{aligned} C(u) = \int_0^\infty \frac{kdk}{4\pi} \Bigg\{ & \frac{X(E_k)}{E_k^5}\left(-\frac{3}{2}\xi_k^2 k^2 + E_k^2 k^2 + \frac{1}{2}\xi_k E_k^2 - \frac{1}{4}u^2 E_k^2\right) \\ & + \frac{\Delta^2 X'(E_k)\, k^2}{E_k^4}\left[\left(\frac{u}{v_k}\right)^2\left(\sqrt{\frac{u^2}{u^2 - v_k^2}} - 1\right) - \frac{1}{2}\right]\Bigg\}. \end{aligned} \tag{23}$$

with $v_k = \partial E_k/\partial k = 2k\xi_k/E_k$ the group velocity of the fermionic (pair-breaking) excitations. The resulting solution u of Eq. 20 is interpreted as the complex sound velocity, as in [13]. Specifically, the real part of is the speed of sound (the sound mode energy divided by q), whereas the negative imaginary part equals the damping rate divided by q.

3. Results and discussion

3.1. Sound mode as pole of the propagator

In expressions (21)-(23) for the coefficients U, D and C, there are terms of the form

$$\mathcal{F}(u) = \int_0^\infty \frac{f(k,u)}{\sqrt{u^2 - v_k^2}}. \tag{24}$$

The denominator $\sqrt{u^2 - v_k^2}$ results in a branch cuts along the real axis for $\mathcal{F}(u)$ in the complex u plane. As we need to obtain U, D and C in the lower complex plane to find solutions of (20), it is necessary to analytically continue these functions through the branch cuts. For this we use the same method as in Refs. [12,13], namely the analytic continuation scheme introduced by Nozières[23]. It is based on computing the spectral function along the real axis

$$\rho(c) = \frac{1}{2\pi i} \lim_{\delta \to 0} \left[\mathcal{F}(c + i\delta) - \mathcal{F}(c - i\delta)\right]. \tag{25}$$

Then in the lower complex plane, the continuation of ρ provides the desired analytic continuation $\mathcal{F}^c = \mathcal{F}(u) + 2\pi i \rho(u)$. The spectral function $\rho(c)$ exhibits a kink at $c = v_b$ satisfying

$$v_b = 4\mu + 6\Delta^2 \left(\mu\Delta^2 + \Delta^2\sqrt{\mu^2 + \Delta^2}\right)^{-1/3} - 6\left(\mu\Delta^2 + \Delta^2\sqrt{\mu^2 + \Delta^2}\right)^{1/3}. \tag{26}$$

The analytic continuation of the spectral function to the left of the kink is different from the continuation of the function to the right of v_b. This divides the analytically continued functions in two, as it effectively rotates the branch cut to the line $[v_b - 0i, v_b - i\infty]$. Hence, there are two regions in the lower complex u plane: domain I with $\mathrm{Re}(u) < v_b$ and domain II with $\mathrm{Re}(u) > v_b$. As in the three-dimensional case, the presence of the two domains has a physical origin: the group velocity v_k corresponds to a Landau critical velocity for emitting fermionic excitations in the superfluid, and v_b is the maximal

group velocity for fermionic excitations with $k < k_F$. For more details on the continuation scheme (in 3D), we refer to [13].

An example of the analytic continuation is shown in Fig. 1, plotting the numerically computed values of $\det \mathbb{M}$ in the lower complex plane. A complex root is present at the point where the white line (where $\mathrm{Im}\,(\det \mathbb{M}) = 0$) and the black line (where $\mathrm{Re}\,(\det \mathbb{M}) = 0$) cross. This root corresponds to the complex sound velocity at the chosen parameters. The vertical red dotted line is the aforementioned branch cut between the two domains. The roots were always sought with an imaginary value of less than 2, because for higher values of $\mathrm{Im}\,(u)$ the collective excitations are overdamped.

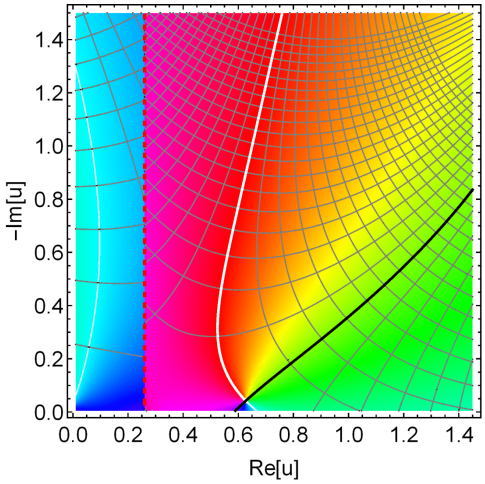

Figure 1. The (complex) determinant of the inverse fluctuation propagator is shown as a function of u, for $E_b = 1.8$ and $\beta = 0.87$. The color reveals the phase (along a color wheel from red over the spectrum to violet and then back to red). Curves show contours of the real and imaginary values.

Changing parameters such as the temperature, we can track how the root of $\det \mathbb{M}$ moves across the complex plane. Fig. 2 shows the paths of the complex sound velocity u when the temperature passes from zero to T_c, the critical temperature at which $\Delta \to 0$.

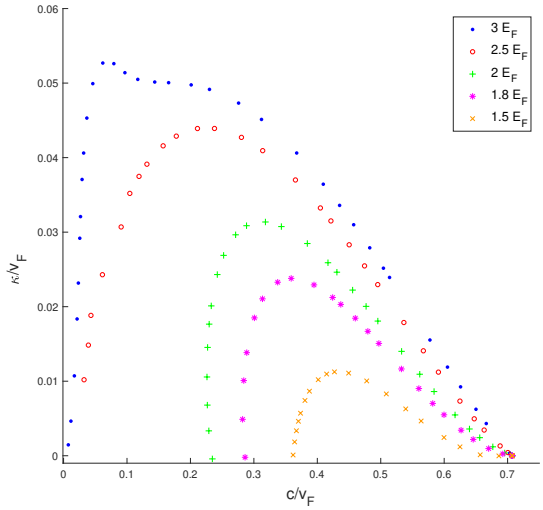

Figure 2. Paths traced by the complex sound velocity when varying temperature from zero to the critical temperature, for different binding energies $E_b = 1.5, 1.8, 2, 2.5, 3(E_F)$.

Various paths for u in the complex plane are shown, corresponding to five different values for the binding energy. At $T = 0$ the results for all binding energies coincide at $u = 1/\left(\sqrt{2}v_F\right)$. This

result is expected for a 2D BCS superfluid, and here we find that it holds for all couplings. This can also be shown analytically by taking the $\beta \to \infty$ limit in expressions (21)-(23). As the temperature is increased towards T_c the paths ends up on the real axis. In the BCS regime, the complex sound velocity disappears below the real axis before the critical temperature is reached. The path for $E_b = 3E_F$ differs from the other paths due to the "bump" at the peak, that we could not yet interpret. In general, a higher binding energy gives a higher damping rate, which is possible because the system in the BEC regime is more dependent on the temperature.

Figs. 3 and 4 show the temperature dependence of the sound velocity $c = \mathrm{Re}(u)$ and the damping parameter $\kappa = -\mathrm{Im}(u)$, respectively. Note that κ equals the damping rate divided by q - just as the energy, the damping rate is linear in q in the long=wavelength limit. The sound velocity decreases monotonically from its zero temperature value of $\sqrt{2}v_F$, but does not reach zero as the temperature reaches the critical temperature.

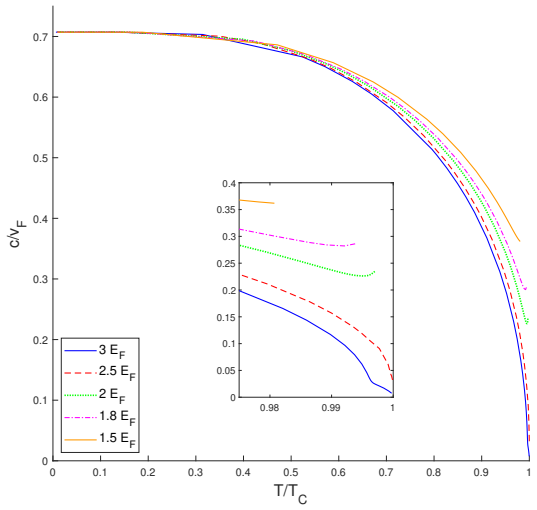

Figure 3. Sound velocity c as a function of temperature for $E_b = 1.5, 1.8, 2, 2.5, 3\,(E_F)$.

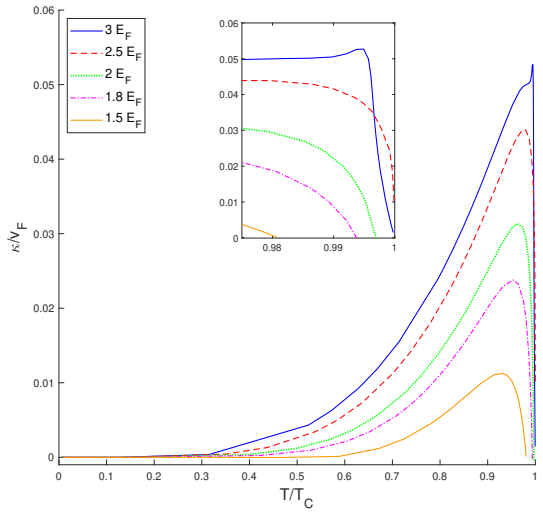

Figure 4. Damping factor κ as a function of temperature for $E_b = 1.5, 1.8, 2, 2.5, 3\,(E_F)$.

The smaller the damping parameter κ is, the more stable the collective excitations are, so that at $T = 0$ we have fully stable excitations. As the temperature rises, as expected, κ also rises, and when

the temperature continues to rise, κ goes down again. In the BEC regime, this result makes sense, since one must view κ relative to c and if κ tends to zero, c also goes to zero. The result that one gets in the BCS regime on the other hand is unexpected, namely a stabilization of the mode close to T_c. This may mean that our description of the system is not accurate at temperatures close to T_c and that the present GPF approximate action for the 2D system is should be restricted to temperatures well below T_c. To get a better estimate of the regime of validity, we investigate the response function in the next subsection.

3.2. Response function

An alternative way to determine the sound velocity, without relying on the analytical continuation, consists in using instead the response function. For low momentum, the pair field response function is given by [13]:

$$q^2\mathbb{M}^{-1}\left(uq,\mathbf{q}\right)=\frac{1}{U(u)C(u)-D(u)^2}\begin{pmatrix}C(u)q^2 & iD(u)q\\ -iD(u)q & U(u)\end{pmatrix}+O(q^4). \tag{27}$$

The dominating term here is proportional to the phase-phase element $(\mathbb{M}^{-1})_{2,2}$. We determine the phase-phase response function in the long-wavelength limit as

$$\chi(c)=\lim_{q\to 0}\frac{1}{\pi}\,\mathrm{Im}\left[q^2(\mathbb{M}^{-1})_{2,2}\left(\left(c+0^+i\right)q,\mathbf{q}\right)\right]=\frac{1}{\pi}\,\mathrm{Im}\left[\frac{U}{UC-D^2}\left(c+0^+i\right)\right] \tag{28}$$

Note that a presence just below the real axis of a pole (i.e. a node of $UC-D^2$) will lead to an peak of $\chi(c)$. The location of the peak approximates the real value of the pole, i.e. to the sound velocity. The height of the peak is determined by the residue, and its width is determined by how far in the lower half plane the pole lies. Hence, the value of c for which the response function achieves a maximum $c\equiv c_{resp}$ can be used as an approximation for the sound velocity.

The numerical solutions for c and c_{resp} lie close to each other, as can be seen from Fig. 5. An advantage of this second technique is that it is more reliable to determine the sound speeds close to T_c, and hence allows us to estimate the region of validity for our results.

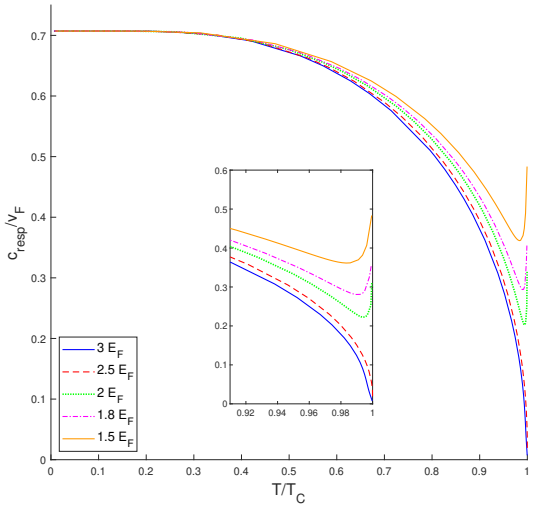

Figure 5. Sound velocity c_{resp} as a function of temperature for $E_b=1.5,1.8,2,2.5,3\,(E_F)$. *Inset*: this sound velocity for temperatures close to T_C.

From Fig. 5, it can be seen that the sound speed starts to rise again close to T_c in the BCS regime. This phenomenon is not intuitively expected and deviates from that of Fig. 3 but can possibly be explained by second sound. The first sound is the sound wave of the density fluctuations. Normally,

temperature differences spread through diffusion, but with second sound we have temperature fluctuations that behave like waves. Second sound only occurs in the Bose condensed state, so it is possible that in the BCS regime the first sound dominates and therefore does not disappear at and above the critical temperature, whereas the BEC regime second sound dominates and therefore disappears at T_c. Regardless of this interpretation, we can identify the region where c corresponds to c_{resp} as the region where the method of finding the sound velocity from the poles of the bosonic fluctuation propagator is reliable. This turns out to be a rather large fraction of the temperature range, $T \lessapprox 0.95\ T_c$.

4. Conclusions

The aim of this work is to determine the long-wavelength dispersion of Anderson-Bogoliubov excitations for two-dimensional superfluid Fermi gases by locating the poles of the propagator of pair field fluctuations. The fluctuation propagator is in turn obtained via an expansion of the matrix elements of the GPF action up to the second order in powers of q. As was the case for the 3D system, our method of analytical continuation does not need to assume that the poles lie close to the real axis (i.e. that the damping can be tackled perturbatively). We found that at $T = 0$, the sound velocity is equal to $v_F/\sqrt{2}$ independently on the binding energy, and the damping rate is equal to zero. As the temperature rises, the sound velocity decreases and the damping increases.

The response function has been calculated for various temperatures and binding energies. The maxima of the response functions could then be used to determine the sound rates at different temperatures and binding energies in an alternative way, which gives almost the same results as those obtained through complex poles of the fluctuation propagator, except the close vicinity of the transition temperature, where the second method is more reliable. The estimated sound velocities agree with the previous results, and we get a better view at the sound velocity near the critical temperature T_c. In the BCS regime, we still have stable collective excitation at T_c, while in the BEC regime this is not the case. The reason for this could be that in the BCS regime first sound dominates and keeps existing past T_c, while in the BEC regime second sound dominates and disappears past T_c.

Recently, the sound mode was studied experimentally for a uniform Fermi superfluid in a box trap. The superfluid was excited at a given frequency by vibrating a wall of the container, and the resulting density response was measured to estimate both the dispersion and the damping. A similar technique could well be employed to study the sound mode in the two-dimensional case, given the versatility of trapping potentials that can be achieved. This could allow to experimentally verify the results predicted here. Finally, we note that the path-integral technique used here has as a specific advantage over some other methods that it explicitly allows to study the sound mode at non-zero temperatures, relevant to the experiments.

Acknowledgments: Discussions with C. A. R. Sá de Melo, A. Perali, H. Tajima and Yu. Yerin are gratefully acknowledged. This work is supported by the University Research Fund (BOF) of the University of Antwerp and by the Flemish Research Foundation (FWO-Vl), project No. G.0429.15.N and the European Union's Horizon 2020 research and innovation program under the Marie Skłodowska-Curie grant agreement number 665501.

1. M. Bartenstein, A. Altmeyer, S. Riedl, S. Jochim, C. Chin, J. H. Denschlag, and R. Grimm, *Collective Excitations of a Degenerate Gas at the BEC-BCS Crossover*, Phys. Rev. Lett. **92**, 203201 (2004).
2. J. Kinast, A. Turlapov, and J. E. Thomas, *Damping of a Unitary Fermi Gas*, Phys. Rev. Lett. **94**, 170404 (2005).
3. A. Altmeyer, S. Riedl, C. Kohstall, M. J. Wright, R. Geursen, M. Bartenstein, C. Chin, J. Hecker Denschlag, and R. Grimm, *Precision Measurements of Collective Oscillations in the BEC-BCS Crossover*, Phys. Rev. Lett. **98**, 040401 (2007).
4. M. K. Tey, L. A. Sidorenkov, E. R. S. Guajardo, R. Grimm, M. J. H. Ku, M. W. Zwierlein, Y.-H. Hou, L. Pitaevskii, and S. Stringari, *Collective Modes in a Unitary Fermi Gas across the Superfluid Phase Transition*, Phys. Rev. Lett. **110**, 055303 (2013).

5. L. A. Sidorenkov, M. K. Tey, R. Grimm, Y.-H. Hou, L. Pitaevskii, and S. Stringari, *Second sound and the superfluid fraction in a Fermi gas with resonant interactions*, Nature (London) **498**, 78 (2013).
6. S. Hoinka, P. Dyke, M. G. Lingham, J. J. Kinnunen, G. M. Bruun, and C. J. Vale, *Goldstone mode and pair-breaking excitations in atomic Fermi superfluids*, Nat. Phys. **13**, 943 (2017).
7. P. B. Patel, Z. Yan, B. Mukherjee, R. J. Fletcher, J. Struck, M. W. Zwierlein, *Universal Sound Diffusion in a Strongly Interacting Fermi Gas*, arXiv:1909.02555.
8. B. Mukherjee, Z. Yan, P. B. Patel, Z. Hadzibabic, T. Yefsah, J. Struck, and M. W. Zwierlein, Homogeneous Atomic Fermi Gases, Phys. Rev. Lett. **118**, 123401 (2017).
9. P. W. Anderson, *Random-Phase Approximation in the Theory of Superconductivity*, Phys. Rev. **112**, 1900 (1958).
10. Y. Ohashi, A. Griffin, *Superfluidity and collective modes in a uniform gas of Fermi atoms with a Feshbach resonance*, Phys. Rev. A **67**, 063612 (2003).
11. *R. Combescot, M. Y. Kagan, S. Stringari, Collective mode of homogeneous superfluid Fermi gases in the BEC-BCS crossover*, Phys. Rev. A **74**, 042717 (2006).
12. H. Kurkjian, S. N. Klimin, J. Tempere, and Y. Castin, *Pair-Breaking Collective Branch in BCS Superconductors and Superfluid Fermi Gases*, Phys. Rev. Lett. **122**, 093403 (2019).
13. S. N. Klimin, J. Tempere, and H. Kurkjian, *Phononic collective excitations in superfluid Fermi gases at nonzero temperatures*, Phys. Rev. A **100**, 063634 (2019).
14. S. N. Klimin, H. Kurkjian, and J. Tempere, Leggett collective excitations in a two-band Fermi superfluid at finite temperatures, New J. Phys. **21**, 113043 (2019).
15. C. A. R. Sá de Melo, M. Randeria, and J. R. Engelbrecht, *Crossover from BCS to Bose superconductivity: transition temperature and time-dependent Ginzburg-Landau theory*, Phys. Rev. Lett. **71**, 3202 (1993)
16. J. R. Engelbrecht, M. Randeria, and C. A. R. Sá de Melo, *BCS to Bose crossover: Broken-symmetry state*, Phys. Rev. B **55**, 15153 (1997).
17. R. B. Diener, R. Sensarma, and M. Randeria, *Quantum fluctuations in the superfluid state of the BCS-BEC crossover*, Phys. Rev. A **77**, 023626 (2008).
18. R. P. Feynman and A. R. Hibbs, *Quantum Mechanics and Path Integrals* (McGraw-Hill, 1965).
19. M. Randeria, J.M. Duan, L.Y. Shieh, "Superconductivity in a two-dimensional Fermi gas: Evolution from Cooper pairing to Bose condensation". Phys. Rev. B 41, 327 (1990).
20. J. Hubbard, *Calculation of Partition Functions*. Phys. Rev. Lett. **3**, 77 (1959).
21. R.L. Stratonovich, *On a method of calculating quantum distribution functions*, Doklady Akad. Nauk S.S.S.R. **115**, 1097 (1957) [Soviet Phys. Doklady **2**, 416 (1958)].
22. J. Tempere, J. P. A. Devreese, *Path-Integral Description of Cooper Pairing*, in *Superconductors – Materials, Properties and Applications*, ed. by A. Gabovich (Institute of Physics, Ukraine, 2012). DOI: 10.5772/48458.
23. P. Nozières, *Le problème à N corps: propriétés générales des gaz de fermions* (Dunod, Paris, 1963).